

# Study on Bandwidth Frequency of Servo Valve based on Metering Cylinder

## 실린더를 이용한 서보 밸브 대역폭 주파수의 측정에 관한 연구

S. D. Kim<sup>1</sup>, Wen-Long An<sup>2\*</sup> and S. H. Jeon<sup>1</sup>

김성동 · 안문용 · 전세형

Received: 10 Aug. 2015, Revised: 1 Sep. 2015, Accepted: 7 Sep. 2015

**Key Words** : Servo Valve (서보밸브), Bandwidth Frequency(대역폭 주파수), Spool Displacement(스풀 변위), Linear Velocity Transducer (선형 속도 변환기)

**Abstract**: In this study, a metering cylinder was constructed, and the velocity obtained from the linear velocity transducer (LVT) of the cylinder piston was used to evaluate the dynamic performance of an electro-hydraulic servo valve. Frequency response experiments involving the spool displacement and piston velocity (LVT signal) were conducted with different input signal amplitudes, hydraulic pipe diameters, and supply pressures. The spool displacement signal accurately reflected the performance of the servo valve. Meanwhile, the -3 dB bandwidth frequency of the LVT signal was similar to the spool displacement signal, except for a small-amplitude input signal, and the -90° phase lag bandwidth frequency showed some differences.

### Nomenclature

$A_p$  : area of piston,  $m^2$

$B_p$  : viscous damping coefficient,  $N \cdot s/m$

$C_d$  : discharge coefficient of orifice, no dimension

$C_{ep}$  : external leakage coefficient of metering cylinder,  $m^3/Pa \cdot s$

$C_{ip}$  : internal leakage coefficient of metering cylinder,  $m^3/Pa \cdot s$

$C_{tp}$  : total leakage coefficient,  $m^3/Pa \cdot s$

$F_L$  : arbitrary load force on piston,  $N$

$K_c$  : flow-pressure coefficient,  $m^3/s/Pa$

$K_q$  : flow gain,  $m^3/s/m$

$M_t$  : total mass of piston and load referred to piston,  $kg$

$P_1, P_2$  : outlet pressures of servo valve,  $Pa$

$P_L$  : load pressure of  $P_1 - P_2$ ,  $Pa$

$Q_L$  : load flow rate,  $(Q_1 + Q_2)/2$ ,  $m^3/s$

$V_1, V_2$  : chamber volumes of metering cylinder,  $m^3$

$V_t$  : total volume of both chambers of cylinder,  $m^3$

$w$  : area gradient of valve port,  $m$

$x_p$  : displacement of piston,  $m$

$x_v$  : spool displacement from neutral,  $m$

$\beta_e$  : effective bulk modulus of system,  $Pa$

$\rho$  : oil density,  $kg/m^3$

\* Corresponding author: awl2013@sina.cn

1 Department of Mechanical System Engineering, Kumoh National Institute of Technology, Gumi 054-478-7395, Korea

2 School of Construction Machinery, Chang'an university, People's Republic of China

Copyright © 2015, KSFC

This is an Open-Access article distributed under the terms of the Creative Commons Attribution Non-Commercial License(<http://creativecommons.org/licenses/by-nc/3.0>) which permits unrestricted non-commercial use, distribution, and reproduction in any medium, provided the original work is properly cited.

### 1. Introduction

In hydraulic fluid power systems, power is transmitted by a fluid under pressure from a

hydraulic power source to one or several loads through electrically modulated hydraulic control valves. The range of applications for electro-hydraulic servo-systems is diverse, and includes manufacturing systems, material test machines, active suspension systems, mining machinery, fatigue testing, flight simulation, paper machines, ships, electromagnetic marine engineering, injection molding machines, robotics, and steel and aluminum mill equipment. A servovalve is a core element of a hydraulic system and directly affects the performance and characteristics of the whole system. There are numerous performance characteristics that must be investigated to successfully apply an electro-hydraulic servovalve. In this paper, we focus on a dynamic property of the servovalve, namely its bandwidth frequency. There are three kinds of dynamic test methods based on different return signals that are recommended by ISO 10770-1<sup>1)</sup>

The first method uses the velocity of a piston driven by a low-friction, low-inertia cylinder as a dynamic flow signal. The second method uses the spool displacement signal of a displacement transducer integrated into the servovalve. Finally, the third method employs an external spool displacement transducer and appropriate signal conditioning electronics for the measured signal.

The valve's spool displacement signal is considered to reflect the real dynamic property of the servovalve because the spool displacement is not affected by environmental conditions such as the effective bulk modulus of the oil, size of the

outlet volume, and size of the actuator.

This work investigated the effectiveness of the method that uses the velocity of the piston as a dynamic flow signal. A low-inertia, low-friction metering cylinder, which is recommended by ISO 10770-1, was constructed, and the piston's velocity was adopted as a return signal to measure the servovalve bandwidth frequency and compare the difference between the first and second methods recommended by ISO 10770-1.

## 2. Description of testing system

The dynamic test system consisted of a power supply, servovalve, metering cylinder, and displacement transducer, as shown in Fig. 1 and Fig. 2. The servo controller compared the signal from the feedback displacement transducer with the input reference signal to determine the displacement error, and produce a command signal to drive the servovalve. The servovalve adjusted the flow of pressurized oil to move the metering cylinder at a speed of  $v$ . Thus, the flow rate can be calculated by the piston's speed using the following equation.

$$Q_L = vA_p \tag{1}$$

The general flow equation for the four-way critical center valve can be written as follows:

$$Q_L = C_d w x_v \sqrt{\frac{P_s - P_L}{\rho}} \tag{2}$$

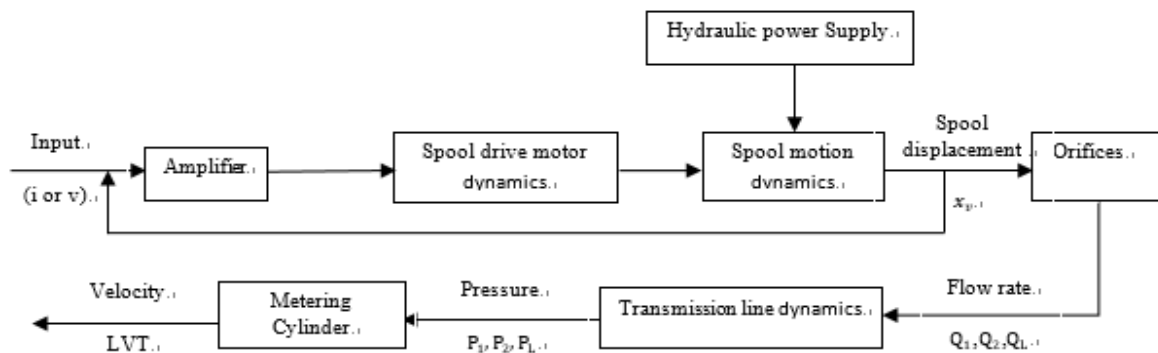


Fig. 1 Schematic block diagram of a servo valve

The linearized equation describing the valve flow becomes

$$Q_L = K_q x_v - K_c P_L \quad (3)$$

Considering leakage flow in the metering cylinder gives the continuity equations for the volumes  $V_1$  and  $V_2$  as follows.

$$\frac{V_1}{\beta_e} \frac{dP_1}{dt} = Q_1 - C_{ip}(P_1 - P_2) - C_{ep}P_1 - \frac{dV_1}{dt} \quad (4)$$

$$\frac{V_2}{\beta_e} \frac{dP_2}{dt} = Q_2 + C_{ip}(P_1 - P_2) - C_{ep}P_2 + \frac{dV_2}{dt} \quad (5)$$

Assume that the piston is in a centered position ( $x_p = 0$ ), and the chamber volumes  $V_1, V_2$  are  $V_t/2$ , where  $V_t$  is the total pressurized volume in the cylinder. The load pressure and load flow rate are defined like following equations.

$$P_L = P_1 - P_2 \quad (6)$$

$$Q_L = (Q_1 + Q_2)/2 \quad (7)$$

Combining equations (4) and (5), and using the definition of the load pressure and load flow rate results in equation (8).

$$Q_L = A_p \frac{dx_p}{dt} + C_{ip}P_L + \frac{V_t}{4\beta_e} \frac{dP_L}{dt} \quad (8)$$

The final equation for the actuator arises from the forces of the piston. The motion equation described by the forces can be written as follows:

$$P_L A_p = M_t \frac{d^2 x_p}{dt^2} + B_p \frac{dx_p}{dt} + F_L \quad (9)$$

If equations (3), (8), and (9) are transformed by the Laplace transformation, the transfer function of  $x_p$  for spool displacement  $x_v$  and the arbitrary load force  $F_L$  on the piston are related as follows:

$$x_p = \frac{\frac{K_q}{A_m} x_v - \frac{K_{ce}}{A_p^2} (1 + \frac{V_t}{4\beta_e K_{ce}} s) F_L}{s (\frac{s^2}{w_h^2} + \frac{2\delta_h}{w_h} s + 1)} \quad (10)$$

In equation (10),  $s$  is the Laplace variable,  $w_h$  is the hydraulic natural frequency, and  $\delta_h$  is the

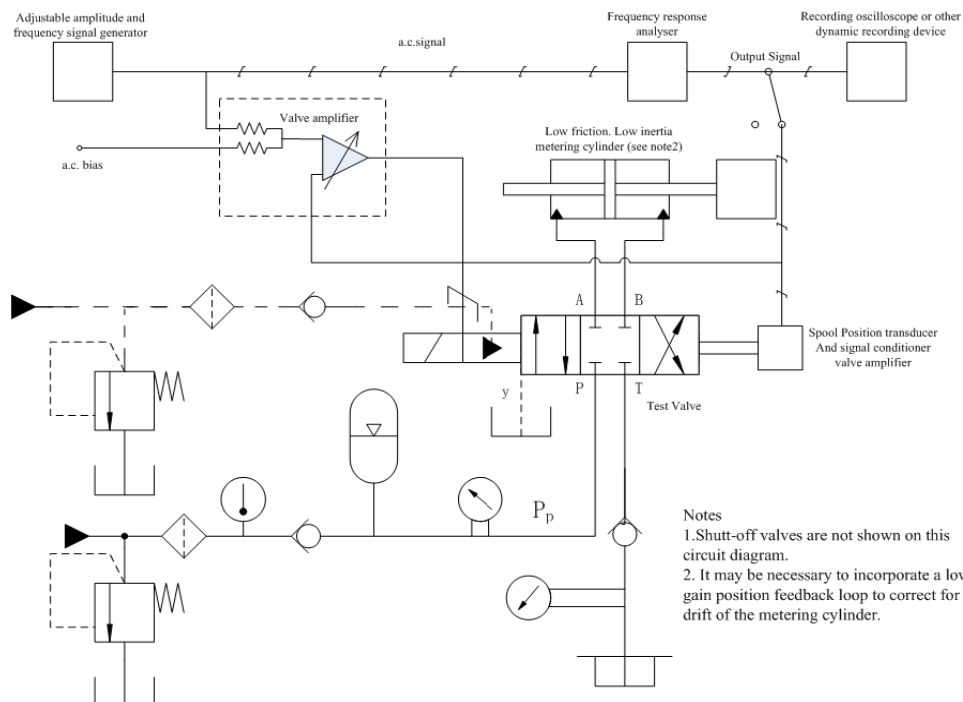


Fig. 2 Typical circuit suggested by ISO 10770-1 to measure dynamic flow rate

hydraulic damping ratio.  $K_{ce}$  is the total flow-pressure coefficient. These parameters are described as the following equations <sup>2)</sup>.

$$w_h = \sqrt{\frac{4\beta_e A_p^2}{V_t M_t}} \quad (11)$$

$$\delta_h = \frac{K_{ce}}{A_p} \sqrt{\frac{\beta_e M_t}{V_t}} + \frac{B_p}{4A_p} \sqrt{\frac{V_t}{\beta_e M_t}} \quad (12)$$

$$K_{ce} = K_c + C_{tp} = K_c + C_{ip} + \frac{C_{ep}}{2} \quad (13)$$

### 3. Design of metering cylinder

In the dynamic test system, the metering cylinder should have low inertia and low friction. Thus, the engineering plastic material, polyether ether ketone (PEEK) was adopted to construct the piston of the cylinder. PEEK <sup>3)5)</sup> is known to have a much lower density and friction coefficient than steel or aluminum. In addition, the rubber seals on the piston were also removed to reduce the friction, while five grooves were machined to reduce the lateral force and prevent internal leakage.

In control theory<sup>6)</sup>, the dynamic behavior of a much faster subsystem can be neglected when its natural frequency is more than three times the characteristic frequency of the dominant dynamic subsystem<sup>1)</sup>. The metering cylinder was designed so that its natural frequency  $w_h$ , as shown in equation (11), was larger than three times the expected bandwidth frequency  $w_{sv}$  of the servovalve.

$$w_h = \sqrt{\frac{4\beta_e A_p^2}{V_t M_p}} \geq 3w_{sv} \quad (14)$$

The stroke of the metering cylinder should be long enough to avoid contacting the end of the cylinder at the lowest frequency for the input to the valve.

$$A_p S \geq 2 \int_0^{\frac{\pi}{w_1}} Q_{max} \sin(w_1 t) dt \quad (15)$$

In equation (15),  $S$  is the stroke of the metering cylinder.  $w_1$  represents the lowest frequency of the servovalve, and  $Q_{max}$  is the flow amplitude of the servovalve.

The transmission line that connects the servovalve and metering cylinder should be as short as possible, while having a suitable diameter, to balance the effect of the capacitance and inertia in the transmission line <sup>7)</sup>.

The metering cylinder that was constructed according to ISO 10770-1 is shown in Fig. 3.

The design parameters of the metering cylinder are listed in Table 1.

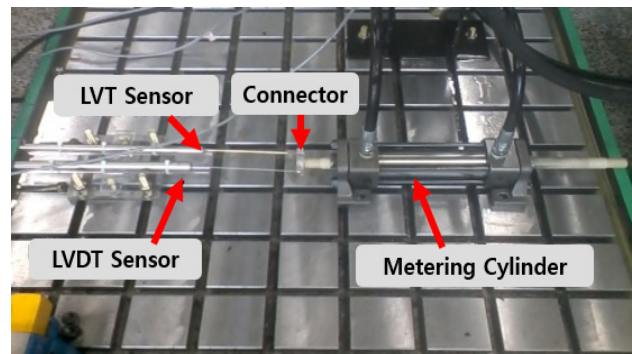


Fig. 3 Photo of metering cylinder

Table 1 Specification of testing system

material and mass $M_p$ of the piston	PEEK, 0.33 kg
$M_t$ : total mass of piston and oil in pipe and cylinder, kg	2.357 kg
area of the piston $A_p$	$1.569 \times 10^{-3} m^2$
ports volume $V_t$ (including line volume)	$2.505 \times 10^{-4} m^3$
effective bulk modulus of oil $\beta_e$	$3.0 \times 10^8 Pa$
predicted bandwidth frequency $w_{sv}$	100 Hz
internal leakage $C_{ip}$	$1 \times 10^{-12} m^3 / Pa \cdot s$
external leakage $C_{ep}$	$1 \times 10^{-18} m^3 / Pa \cdot s$
absolute viscosity $\mu$	$1.48 \times 10^{-2} N \cdot s / m^2$
flow-pressure coefficient $K_c$	$9.238 \times 10^{-13} m^3 / Pa \cdot s$
total flow-pressure coefficient $K_{ce}$	$1.424 \times 10^{-12} m^3 / Pa \cdot s$
viscous friction coefficient $B_p$	$2 \times 10^3 N \cdot s / m$
area gradient of valve ports $w$	$5.8 \times 10^{-3} m^2 / m$
radial clearance between spool and sleeve $c$	$4.9 \times 10^{-6} m$
discharge coefficient $C_d$	0.61 dimensionless
cylinder natural frequency $w_h$	356 Hz
stroke of piston $s$	150 mm
oil density	$867 kg / m^3$
maximum flow rate $Q_{max}$	$3.33 \times 10^{-4} m^3 / s$

The metering cylinder's natural frequency was designed to fit equation (14) and was calculated to be 356 Hz. In the design process for the natural frequency  $w_h$ , the mass  $M_t$  included not only the piston mass but also the inertia of the oil in the hydraulic cylinder and transmission line. The effective bulk modulus of oil  $\beta_e$  was also chosen in a very conservative manner. Assuming that some air was entrapped inside the oil and the hydraulic hose was very flexible, a low value of  $3.0 \times 10^8$  Pa was selected for the effective bulk modulus of the oil  $\beta_e$ . When the bandwidth frequency of the servovalve was anticipated, the real natural frequency did have the characteristic shown in equation (14).

When the frequency of  $\omega_1$  is chosen to be 1 Hz, the minimum chamber volume of the cylinder should be larger than  $2.12 \times 10^{-4} \text{ m}^3$  according to equation (15). The real internal volume of the metering cylinder is  $2.35 \times 10^{-4} \text{ m}^3$ , which is the product of the area and stroke of the piston. Thus, the design of this metering cylinder is reasonable.

#### 4. Experiment results

The entire dynamic test apparatus was setup as shown in Fig. 4, and the detailed specifications are listed in Table 2.

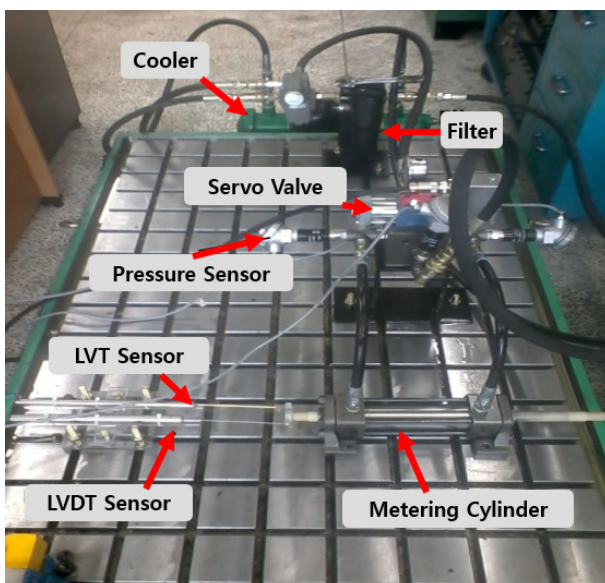


Fig. 4 Photo of dynamic flow rate test

Hydraulic pipes with diameters of  $\frac{1}{2}$  inch (12.7 mm),  $\frac{3}{8}$  inch (9.53 mm), and  $\frac{1}{4}$  inch (6.35 mm) were used to connect the servovalve and metering cylinder. Sine wave signals with differential amplitudes (1 V, 2.5 V, 5 V, 7.5 V, and 9 V) were input to the servovalve at supply pressures of 70 bar and 100 bar.

Some of the results of the series of experiments are shown in Fig. 5.

Table 2 Specifications of dynamic flow test system

Instruments	Specification	Model Number
Servovalve	10 [Lpm]	MOOG D633-317B
Power unit	10 [Lpm]	Shimadza SGP2-52R040
PC	2.0 GHz 504 MB of RAM	National Instrument NI-PXI-1031
DAQ board	Resolution 16 bit, A/D16, D/A 2	National Instrument NI-PXI-6251 M Series
BNC connector	-	National Instrument NI-BNC-2120
Pressure sensor	0-200 [bar] 1-5 V [VDC] Hysteresis 0.025%	Sensys PSHE0100BXHG
Reducing pressure valve	35-140 [bar] 50 [Lpm]	SEWON-Yuken RCT-03-C-22
Water cooler	100LTS	DHC
Filter	10 $\mu\text{m}$ , 12.7 gpm	MP Filter FHP065-1-A1-0-AN
Measurement software	LabVIEW 2012	National Instrument LabVIEW
LVT	21.35 V/(m/s)	TRANS TEK 0264-00005
Linear variable differential transducer(LVDT)	100 mm	TRANS TEK 0114-0000

The first column of Fig. 5 shows the time domain responses of the spool displacement and LVT signal for the sinusoidal valve input. The LVT signal from the metering cylinder's piston represents the dynamic flow rate of the servovalve. The second and third columns show the frequency responses of the servovalve's spool displacement and LVT signal, which are used for Bode plots. The last row shows the bandwidth frequencies with a magnitude of  $-3$  dB and  $-90^\circ$  phase lag for various pipe sizes and supply pressures.

Based on these figures, we find that the  $-3$  dB magnitude bandwidth frequencies of the spool

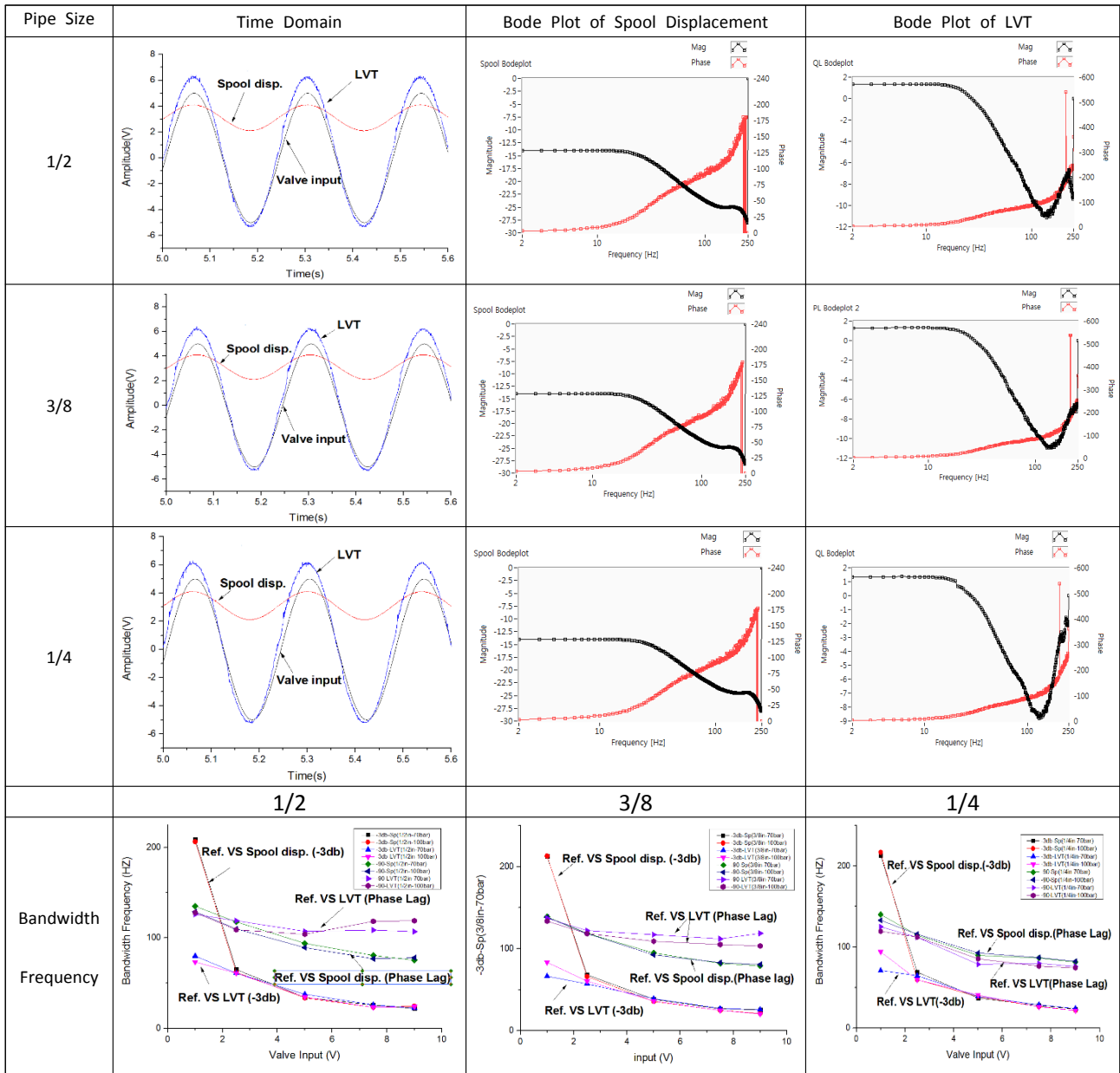


Fig. 5 Experiment results of spool displacement and LVT signal

displacement and LVT signal are very close to each other, except when the input amplitude is 1 V. The -3 dB frequency of the spool displacement for a 1 V input is remarkably high. This phenomenon can also be observed in Fig. 6. It is estimated that this occurs because the servo-amplifier that is built into the servovalve has non-linear characteristics for the saturation limit.

When the spool displacement error for a small input is also small, the amplifier's output is not saturated for the high-frequency range. On the other hand, when the input is more than 2.5 V, the

servo-amplifier is easily saturated for a frequency range that is not very high. The -3 dB frequencies of the LVT or dynamic flow signal agreed well with those of the spool displacement when the input was larger than 1 V, and the spool displacement frequency was lower than 100 Hz. Meanwhile, the -3 dB frequencies of the LVT for the 1-V input were 70~90 Hz and showed a large difference compared to the -3 dB frequencies of the spool displacement, which were around 220 Hz. Even though the metering cylinder used to measure the servovalve's bandwidth frequency was designed

to have a natural frequency of 356 Hz, it was found that the cylinder could not be used to measure the bandwidth frequency of 220 Hz.

The  $-90^\circ$  phase bandwidth frequencies of Fig. 5 and Fig. 7 have the opposite tendency of the  $-3$  dB bandwidth frequency. When the input signal was small (1 V), the  $-90^\circ$  bandwidth frequencies of the LVT signal were nearly the same as the frequencies of the spool displacement. However, the  $-90^\circ$  bandwidth frequencies of the LVT signal showed a larger difference from the frequencies of the spool displacement as the input size increased.

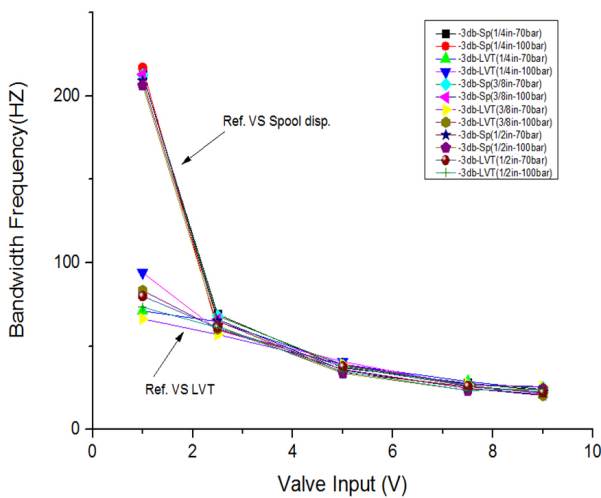


Fig. 6  $-3$  dB bandwidth frequencies of spool displacement and LVT signal on different conditions

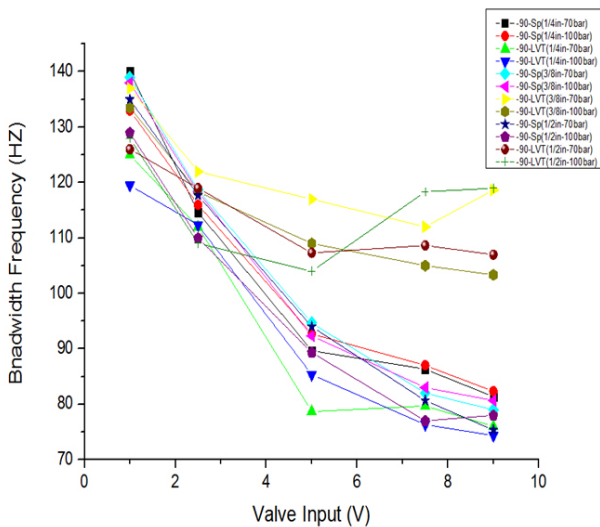


Fig. 7  $-90^\circ$  bandwidth frequency of spool displacement and LVT signal on different conditions

Fig. 6 shows the  $-3$  dB bandwidth frequencies of the “input signal vs. spool displacement” and “input signal vs. LVT” for various supply pressures and transmission-line diameters. Based on this figure, the supply pressure and transmission line diameter are found to have very little effect on the  $-3$  dB bandwidth frequency.

Fig. 7 shows the  $-90^\circ$  phase bandwidth frequencies of the “input signal vs. spool displacement” and “input signal vs. LVT” for various supply pressures and transmission-line diameters. We can find that when the hydraulic pipe is small, the  $-90^\circ$  phase bandwidth frequencies of the “input signal vs. spool displacement” and “input Signal vs. LVT” are close to each other.

### 5. Conclusion

The metering cylinder was designed to have more than three times of the expected bandwidth of a servo valve and a series of experiments were conducted. The follows are the major conclusion deduced from the test results.

(1) The  $-3$  dB bandwidth frequencies of the spool displacement and LVT signal were very similar when the measured bandwidth is lower than one third of the designed natural frequency of the metering cylinder. In addition, they were almost unaffected by the supply pressure and transmission line diameter.

(2) In contrast, the  $-90^\circ$  phase lag bandwidth frequencies of the displacement and LVT signal were close for the small amplitude signal. The  $-90^\circ$  frequencies of the LVT signal showed a larger difference from the frequency of the spool displacement as the amplitude of input increased more.

(3) The experimental results showed that the design of the metering cylinder was reasonable, and could be used to measure the dynamic property of the servovalve relatively well. However, the metering cylinder should be designed to have a hydraulic natural frequency that is triple the anticipated frequency of the servovalve.

## Acknowledgement

This research was supported by Basic Science Research Program through the National Research Foundation of Korea (NRF) funded by the Ministry of Education (2012R1A1A2041242).

## References

- 1) ISO 10770-1 Hydraulic fluid power-Electrically modulated hydraulic control valves - Part 1: Test methods for four-way directional flow control valves, 1998.
- 2) H. E. Merritt, Hydraulic Control Systems, John Wiley & Sons, New York · Chichester· Brisbane · Toronto, 1966.
- 3) Wikipedia, The Free Encyclopedia, <https://en.wikipedia.org/wiki/PEEK>
- 4) D. Kemmish, "Update on the Technology and Applications of Poly Aryl Ether Ketones", ISBN 978-1-84735-408-2, 2010.
- 5) Material Properties Data: Poly ether etherketone (PEEK), [www.makeitfrom.com](http://www.makeitfrom.com)
- 6) K. Ogata, Modern Control Engineering, Prentice-Hall, Inc., Englewood Cliffs, N.J., 1970
- 7) M. Rabie, Fluid Power Engineering, McGraw-Hill Professional, 2009.
- 8) D-Y. Tian, Technology of Electro hydraulic Servovalve, Aviation Industry Press, Beijing, 2008.
- 9) S. D. Kim, S. H. Jeon, and K. H. Jin, "Simulation Study on the Phase Lag Characteristics of Servo valve," Proceedings of the KSFC 2014 Spring Conference, 2014.
- 10) J. Pan, "The Frequency Bandwidth in AGC System Limited by Rated Frequency of Oil Cylinder" Iron and Steel, 1985.
- 11) Y.-B. Liu, "Research on Hydraulic Inherent Frequency of Cylinder," Coal and Mine Machinery, 2013.
- 12) S. Li and Y. Song, "Dynamic Response of a Hydraulic Servo-Valve Torque Motor with Magnetic Fluids," Mechatronics, 2006.
- 13) S. Wu, Z. Jiao, L. Yan, R. Zhang, J. Yu, and C.-Y. Chen, "Development of a Direct-Drive Servo Valve with High-Frequency Voice Coil Motor and Advanced Digital Control," ASME Transactions on Mechatronics, 2014.
- 14) J. Y. Alaydi, "Modeling and Simulation of High-Performance Symmetrical Linear Actuator," International Journal of Scientific & Engineering Research, Volume 3, Issue August 2012.